

Search for Remnant Clouds Associated with the TW Hya Association *

Kengo TACHIHARA †

*Department of Earth and Planetary Sciences, Graduate School of Science, Kobe University,
1-1 Rokko-dai, Nada-ku, Kobe, 657-8501, Japan*

tatihara@kobe-u.ac.jp

Ralph NEUHÄUSER

*Astrophysikalisches Institut und Universitäts-Sternwarte Jena, Schillergäßchen 2-3, D-07745, Jena, Germany
rne@astro.uni-jena.de*

and

Yasuo FUKUI

*Department of Astrophysics, Nagoya University, Chikusa-ku, Nagoya, 464-8602, Japan
fukui@phys.nagoya-u.ac.jp*

(Received ; accepted 2009 March 4)

Abstract

We report on a search for the parental molecular clouds of the TW Hya association (TWA), using CO emission and Na I absorption lines. TWA is the nearest young (~ 50 pc; ~ 10 Myr) stellar association, yet in spite of its youth, there are no detection of any associated natal molecular gas, as is the case for other typical young clusters. Using infrared maps as a guide, we conducted a CO cloud survey toward a region with a dust extinction of $E(B - V) > 0.2$ mag, or $A_V > 0.6$ mag. CO emission is detected toward three IR dust clouds, and we reject one cloud from the TWA, as no interstellar Na absorption was detected from the nearby Hipparcos stars, implying that it is too distant to be related. The other two clouds exhibit only faint and small-scale CO emission. Interstellar Na I absorptions of Hipparcos targets, HIP 57809, HIP 64837, and HIP 64925 (at distances of 133, 81, and 101 pc, respectively) by these clouds is also detected. We conclude that only a small fraction of the interstellar matter (ISM) toward the IR dust cloud is located at distance less than 100 pc, which may be all that is left of the remnant clouds of TWA; the remaining remnant cloud having dissipated in the last ~ 1 Myr. Such a short dissipation timescale may be due to an external perturbation or kinematic segregation that has a large stellar proper motion relative to the natal cloud.

1. Introduction

Kastner et al. (1997) examined a few young stars near the classical T Tauri star, TW Hya (which has become known as the TW Hya association), and suggested that they are nearby and of a young age. Later Hipparcos parallaxes measurements towards TW Hya and HD 98800 yielded a distance of ~ 50 pc, and an age of ~ 10 Myr, although the cluster age and its dispersion are still unclear (Tachihara et al. 2003). The stellar population number of TWA has expanded after a ROSAT X-ray survey and other followup measurements (e.g., Webb et al. 1999), and the current population of the association now comprises more than 20 stars (Zuckerman et al. 2001; Webb 2001).

The proximity of TWA makes it an ideal source for studying faint objects such as: extra-solar planets, proto-planetary disks, and young brown dwarfs (Neuhäuser et al. 2000). Notably however, despite its young age, no molecular cloud remnants from the formation of TWA have been found.

The ROSAT all sky survey and its follow-up optical observations have been successful in finding a large number

of T Tauri stars at a range of distances to their nearest molecular cloud (e.g., Neuhäuser 1997). At this stage, the process by which a T Tauri star becomes separated from its nursery molecular cloud is unclear; one plausible scenario postulates that the young stars are formed in relatively small clouds which are rapidly dissipated (Mizuno et al. 1998; Tachihara et al. 2001; Tachihara et al. 2005). In general however, young stars are found to be closely associated with their natal molecular clouds. For example, Taurus, Chamaeleon, and Lupus 3, whose ages are a few, 5, and a few $\times 10$ Myr, respectively, are all associated with a rich molecular cloud or envelope. An older example, the Pleiades (125 Myr) on the other hand, is not associated with any molecular gas.

A notable young exception is the η Chamaeleontis cluster (~ 8 Myr) at ~ 97 pc, which has no surrounding molecular gas despite its young age (Mamajek et al. 1999; Mizuno et al. 2001). Mamajek et al. (2000) proposed that the η Cha and TW Hya clusters were formed as parts of Sco-Cen OB association and later dispersed with relatively large proper motion. The proximity of TWA makes it better target for exploring this scenario in detail, as a search for remaining faint and small remnant clouds can be made more easily.

As the star formation efficiency for typical star forming

* ESO run ID: 071.C-0568

† Present address: National Astronomical Observatory of Japan, 2-21-2, Mitaka, Tokyo, 181-8588, Japan; k.tachihara@nao.ac.jp

regions (SFRs) is much less than 50%, where the remaining molecular gas is returned to the ISM, the study of the dissipation of molecular gas is an important stepping-stone in the overall objective of understanding matter cycling in the Galaxy. The largest and most extensive molecular cloud survey in our Galaxy is the CfA CO survey (e.g., Dame et al. 2001). However, this survey does not cover the distribution of the TWA members and it is not of sufficient sensitivity to detect the expectedly faint CO of the TWA molecular cloud remnant.

2. Observations

We have made a search for any remnant natal molecular cloud associated with TWA using the CO ($J=1-0$) emission line at 115.2712 GHz and NaI doublet absorption lines at $\lambda = 5889.95 \text{ \AA}$ and 5895.92 \AA . TWA subtends an approximate $40^\circ \times 30^\circ$, and we limit the survey size by using the the IRAS far-IR survey data as a guide map; Fig. 1 shows a dust extinction map of $E(B-V)$ derived from IRAS $100 \mu\text{m}$ and COBE/DIRBE $240 \mu\text{m}$, as demonstrated by Schlegel et al. (1998). We note that some infrared cirrus clouds are located above the Galactic plane where TWA-member stars are distributed. However, these clouds do not appear to spatially correlate with the TWA-member stars. The typical age of TWA stars is $\sim 20 \pm 10$ Myr (Kastner et al. 1997; Jensen et al. 1998), and TWA members with proper motion of 1 km s^{-1} will travel ~ 10 pc (~ 11 deg) since their formation, effectively separating them from the natal clouds. As such, we focus on relatively intense and large IR cirrus clouds, not biased onto spatial correlation of a TWA-member. We instead selecting IR cirrus clouds whose $E(B-V)$ peaks are greater than 0.2 mag (corresponding to $A_V > 0.6$ mag, assuming the empirical relation of $A_V = R_V E(B-V)$ with $R_V \simeq 3.1$). We identify one large and intense cloud, and two diffuse and extended clouds above $b > 15$ deg that contain several local peaks. Hereafter, we refer to these three prominent IR cirrus clouds shown in Fig. 1 as cloud A, B, and C.

2.1. CO observations

^{12}CO ($J=1-0$) observations were conducted with the 4m NANTEN radio telescope at Las Campanas observatory in Chile. At 115 GHz, NANTEN has a beam FWHM of 2.6 arcmin, and a velocity resolution of $\sim 0.1 \text{ km s}^{-1}$. Regions where the dust $E(B-V) > 0.2$ mag were quickly surveyed with a 4-arcmin grid spacing, to a rms sensitivity of ~ 0.2 K. Resulting regions containing a possible CO detection were resurveyed to improve the sensitivity to < 0.1 K. These observations were made with a frequency-switching technique, using a throw interval of 13 – 20 MHz depending on atmospheric condition. A position-switching technique was used instead for clouds with a V_{LSR} close to the telluric CO line. In total, 764 positions were observed.

2.2. NaI observations

We check the physical association of the target molecular clouds with TWA through a distance comparison: TWA-member stars have a distance range of 30 to 120 pc (Frink 2001). Therefore, any background stars in the same line of sight of the clouds, and with a distance of $d \geq 120$ pc should be measurably extinguished by the candidate natal clouds. We selected 21 Hipparcos stars with a parallactic distances $d < 150$ pc, located in and around high dust column density regions of cloud A–C. These were observed with the European Southern Observatory (ESO) 2.2m telescope using the FEROS (Fiber-fed Extended Range Spectrograph). The spectrum range of FEROS spans 3600 to 9200 \AA , and has a resolving power or $R = 48000$ (2 pixels resolution). The standard MIDAS pipeline was used for bias subtraction, flat-fielding, scattered light removal, sky background subtraction and wavelength calibration.

3. Results

3.1. CO survey

The Integrated CO intensity map and the $E(B-V)$ map for cloud A is shown in Fig 2, where we see relatively strong CO emission and its intensity distribution is generally similar to that of dust with $A_V > 0.84$. Notably however, the strong dust peak at $l \sim 280.6$, $b \sim 13.5$ is weakly represented in the CO map. Conversely, the second strongest dust peak at $l \sim 281.5$, $b \sim 14.5$ is strongly represented in the CO map. In addition, we find another CO peak located between the two dust peaks. The peak CO integrated emission is 9.6 K km s^{-1} , corresponding to a molecular hydrogen column density of $1.5 \times 10^{21} \text{ cm}^{-2}$ (Hunter et al. 1997). This is roughly consistent with that derived from the dust A_V (~ 1.1 mag), assuming all the hydrogen is in the molecular form, i.e., $N(\text{H}_2)/A_V = 10^{21} \text{ cm}^{-2} \text{ mag}^{-1}$ (Bohlin et al. 1978).

In contrast to cloud A, CO emission is detected from only small and weak regions in clouds B and C (Figs. 3 and 4). In total, emission with $W(\text{CO}) > 0.3 \text{ K km s}^{-1}$ was measured at only 37 positions from total of 436 points, as shown in Figs. 3 and 4. Table 1 lists the properties of the brightest three $W(\text{CO})$ peaks each from clouds B and C. The dust maps for these two clouds shows a complex morphology, with several column density peaks having $A_V > 0.6$ mag.

CO emissions are detected only toward the three of many peaks of cloud B. In contrast, CO was detected towards all the three dust peaks of cloud C. The correlation between dust A_V and CO intensity is generally weak. The CO spectra towards both clouds B and C, shown in Figs. 3 and 4, are generally complex and have a number of velocity components. The systemic velocity of the CO emission components range between -9 to $+1 \text{ km s}^{-1}$ in cloud B, and from -8 to -5 km s^{-1} in cloud C. These velocities are slightly smaller than the mean V_{LSR} of the TWA stars, at $+2.8 \text{ km s}^{-1}$ (Torres et al. 2003). Additionally worthy of note, is that the V_{LSR} of the CO emission peaks are more dispersed than velocity dispersion of the TWA-member

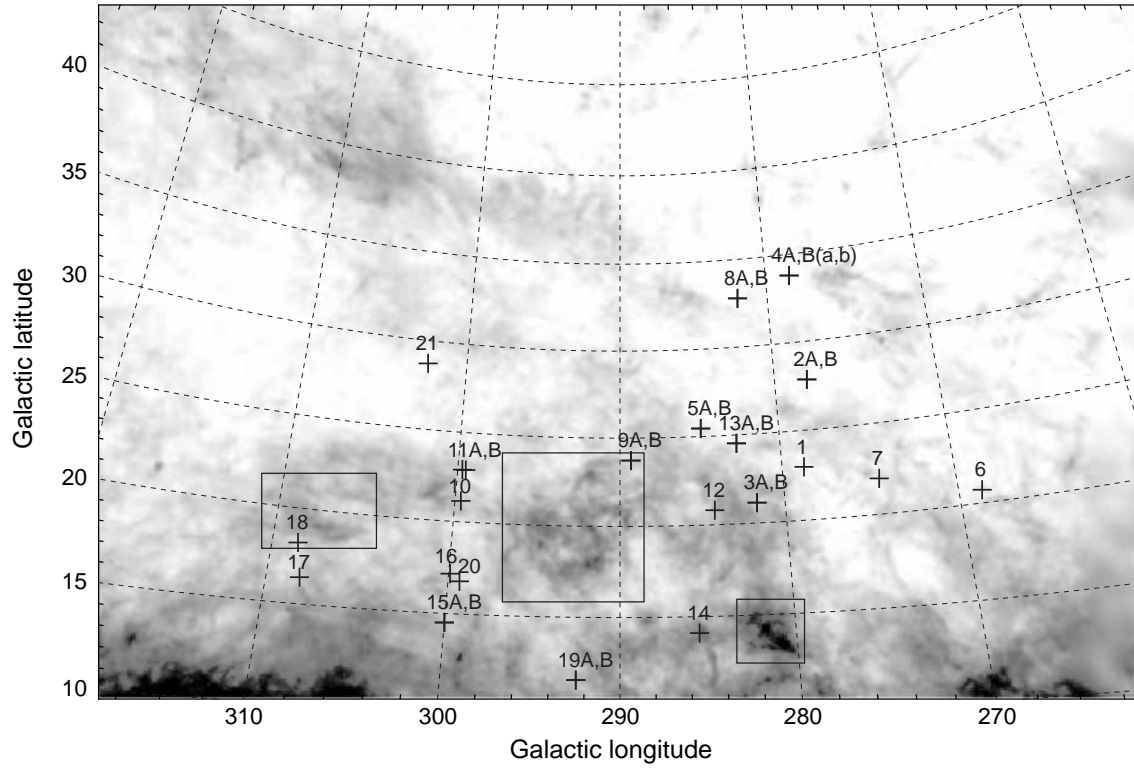


Fig. 1. Far-IR dust A_V map derived from IRAS 100 μm and COBE/DIRBE 240 μm surveys (Schlegel et al. 1998). The TWA stars are shown by crosses with numbers. Three boxes designate the IR cirrus clouds named cloud A, B, and C from right to left.

Table 1. Properties of CO peaks

name	Galactic		R.A.	Decl.	$W(\text{CO})$	peak T_r^*	V_{LSR}^*	ΔV^*	$N(\text{H}_2)^\dagger$
	longitude	latitude	(J2000.0)	(J2000.0)	(K km s $^{-1}$)	(K)	(km s $^{-1}$)	(km s $^{-1}$)	(10^{20} cm $^{-2}$)
B1	289.4667	20.2667	11 44 18.3	-40 50 35	0.32	0.27	-8.5	0.9	0.5
B2	291.4000	18.1333	11 50 49.8	-43 22 38	0.57	0.32	-0.8	1.1	0.9
B3	294.6000	18.6667	12 07 48.1	-43 29 53	0.93	0.75	1.0	1.2	1.5
C1	306.2667	18.6000	13 09 04.0	-44 09 27	2.02	1.71	-7.0	0.9	3.2
C2	306.8667	19.0000	13 12 02.3	-43 42 51	0.51	0.26	-5.0	1.5	0.8
C3	307.4667	19.0667	13 15 07.7	-43 35 47	0.90	0.31	-8.3	2.4	1.4

*Derived by fitting to the gaussian profiles.

† Assuming the conversion factor $N(\text{H}_2)/W(\text{CO})$ of 1.56×10^{20} cm $^{-2}$ (K km s $^{-1}$) $^{-1}$ (Hunter et al. 1997).

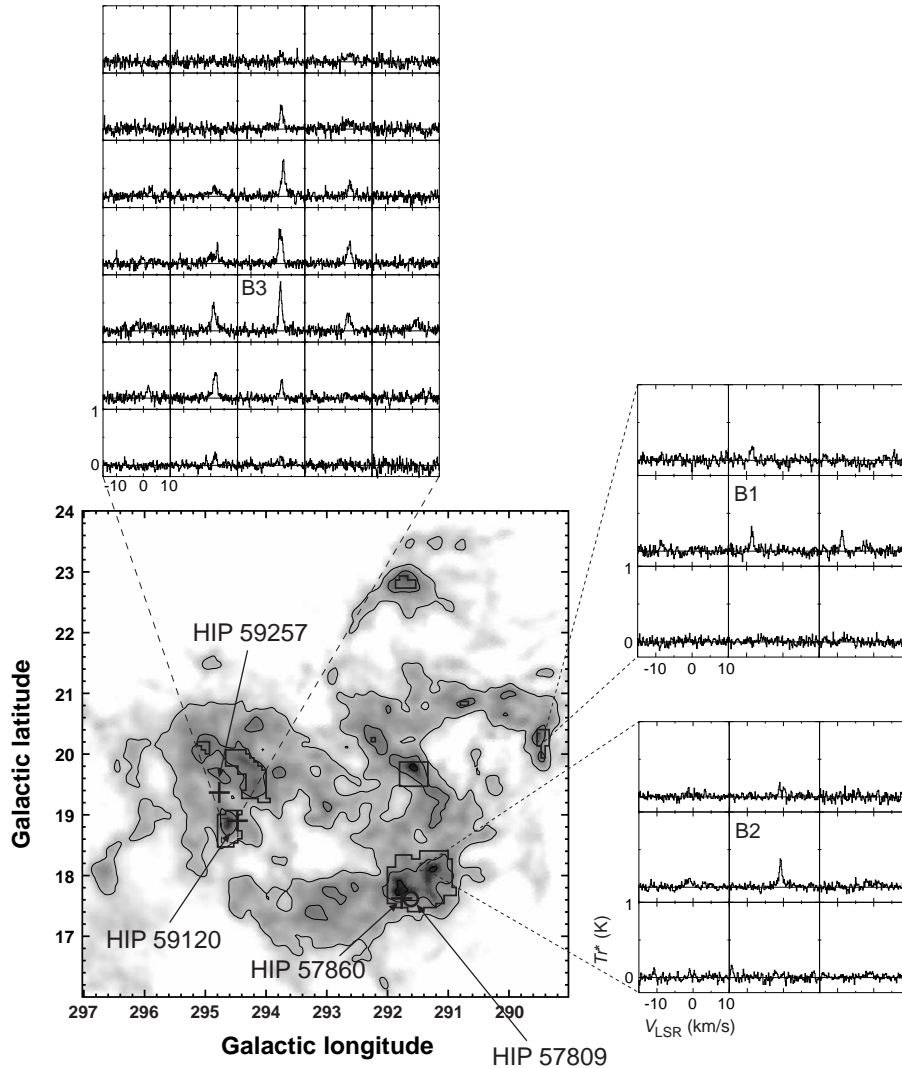


Fig. 3. Main: The dust $E(B-V)$ map of cloud B. Contour intervals are $0.15+0.05$ mag and the crosses indicated the position of the observed Hipparcos stars. Aside: Spectral maps for the three detected CO peaks. CO peak positions listed in Table 1 are labeled. The circle shows the position of HIP 57809 that shows interstellar Na absorption, while crosses are other HIP stars without Na detections.

stars (1.9 km s^{-1} as a standard deviation).

3.2. Optical spectroscopy

To help distinguish the blended NaI stellar emission lines and interstellar absorption lines, we have defined an absorption detection according to the following three criteria: (a) Both of the Na doublet lines have two (partially) resolved components; (b) the interstellar lines are significantly narrower than the stellar ones; (c) the star is not a spectroscopic binary, according to many other absorption lines in the spectrum. Applying these criteria result in the detection of interstellar NaI D absorption of three targets; HIP 57809, HIP 64837, and HIP 64925 (Fig. 5). Targets HIP 57809 and HIP 64837 are towards clouds B and C, respectively, and HIP 64925 is located ~ 2 degrees away from cloud C. The parallactic distances for HIP 57809, HIP 64837 and HIP 64925 are 133, 81, and 101 pc, respectively. We do not detect absorption for any targets

towards cloud A.

The equivalent width, $W(\text{Na})$ and V_{LSR} (calculated from the central wavelength) of the interstellar lines were estimated by fitting a double-component gaussian. To avoid confusion with atmospheric lines, we estimate $W(\text{Na})$ from the D2 line only. After de-blended from the stellar absorption lines we estimate a $W(\text{Na})$ of 0.01, 0.04, and 0.01 \AA and V_{LSR} of 13.6, -1.4 , and -2.5 km s^{-1} for HIP 57809, HIP 64837, and HIP 64925, respectively. The optical spectral resolution relative to the radial velocity is 6.1 km s^{-1} , which is poorer than that obtained from the radio observations.

4. Discussion

4.1. Distance to the clouds

We use the Na absorption lines to constrain the distance to the three clouds. Nine Hipparcos stars with spectro-

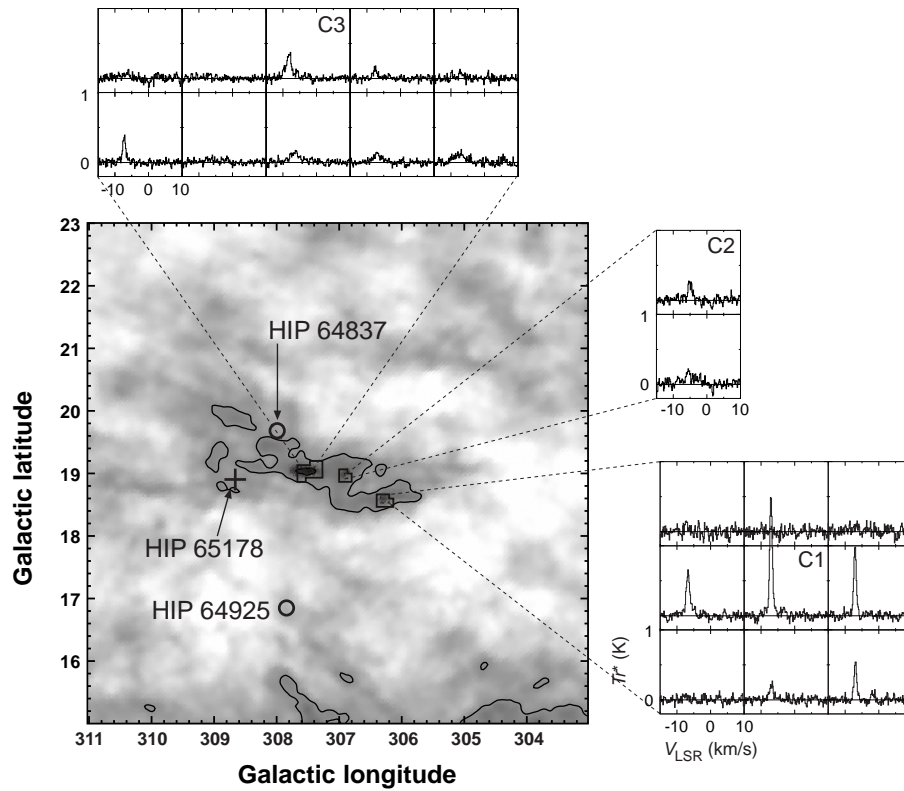


Fig. 4. Main: The dust $E(B - V)$ map of cloud C. Contour intervals are $0.15+0.05$ mag and the crosses indicated the position of the observed Hipparcos stars. Aside: Spectral maps for the three detected CO peaks. CO peak positions listed in Table 1 are labeled. The circles show the positions of HIP 64837 and HIP 64925 that show interstellar Na absorption, while the cross is HIP 65178 without Na detection.

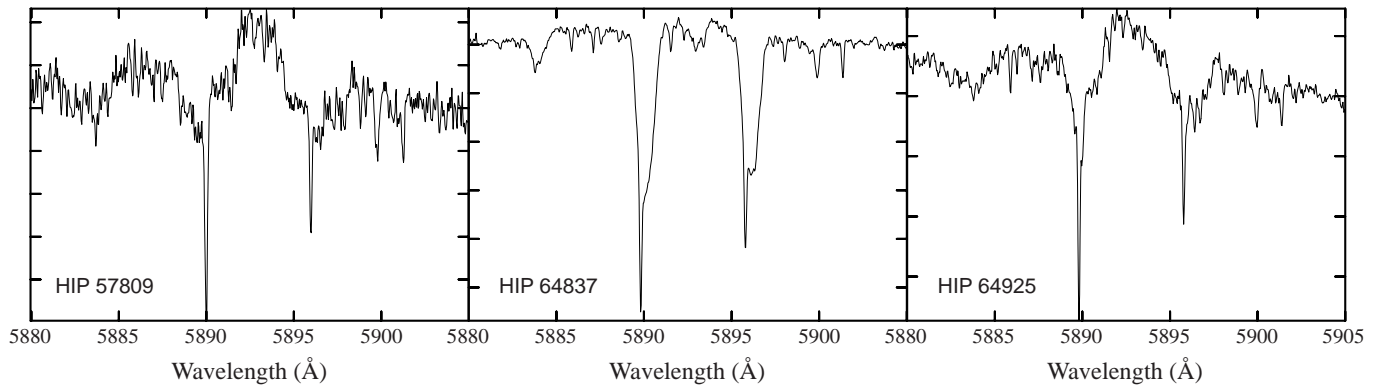


Fig. 5. Optical spectra of HIP 57809, HIP 64837, and HIP 64925. The ordinate is the normalized relative intensity. They all show composite Na absorption lines that consist of wide stellar components and narrow interstellar ones. The intensities are in arbitrary scales.

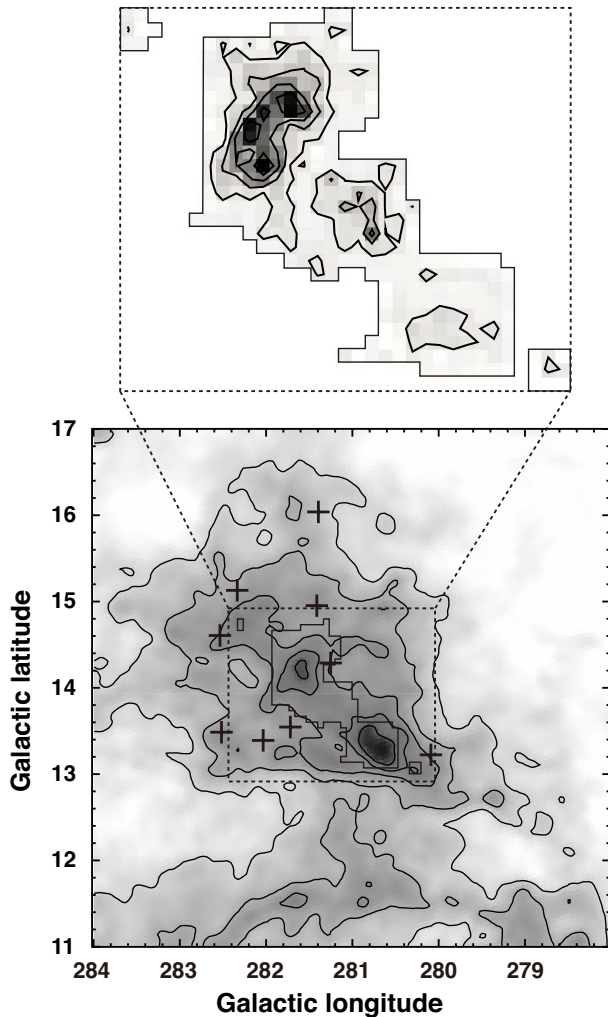


Fig. 2. Bottom: Dust $E(B-V)$ map of cloud A. Contour intervals are $0.15+0.05$ mag and the crosses indicate the positions of the observed Hipparcos stars. Top: CO integrated intensity map of cloud A, over the region indicated in the dust map below. The solid lines indicate the limits of the CO surveyed region. Contour intervals are $1.7+1.7$ K km s $^{-1}$.

scopic data are in the direction of cloud A, however none of these show evidence for absorption, thus the distance of the molecular cloud is likely to be greater than that of the nine stars, specifically, $D_A > 144$ pc. The mean distance of TWA-members is much less than this, and so we conclude that cloud A is not associated with the TWA. The total cloud mass is derived is estimated by $\frac{M}{M_\odot} = 67.5 \left(\frac{d}{150 \text{ pc}}\right)^2$.

Determining the distances to clouds B and C is complicated by their fragmentary morphology. Four Hipparcos stars were observed towards cloud B and only one of them, HIP 57809 ($d = 133$ pc), shows interstellar absorption. A nearby star ($d = 92$ pc), HIP 57860, does not show evidence for absorption. We can thus constrain the distance to cloud B (and more specifically the dust peak at $l \sim 291.^\circ 8$, $b \sim 17.^\circ 7$ east of the CO peak B2) to $92 \text{ pc} < D_{B2 \text{ east}} < 133$ pc. The remaining two stars (HIP 59120 and HIP 59257, at distances of 108 and 76 pc, re-

spectively) do not show interstellar absorption, and so we can further constrain the distance estimate for the peak at $l \sim 294.^\circ 5$, $b \sim 19$ to $D_{B3} > 108$ pc. It is worth mentioning that the velocity of the interstellar absorption toward HIP 57809 ($V_{\text{LSR}} = +13.6$ km s $^{-1}$) is which is significantly larger than that of CO emission at the nearby peak B2 ($V_{\text{LSR}} = -0.8$ km s $^{-1}$), suggesting two layers of ISM in the line of sight. Large difference in V_{LSR} of the three CO peaks (from -8.5 to $+1.0$ km s $^{-1}$) also imply multiple components.

Cloud C shows similar level of complexity: Two Hipparcos stars are located close to this cloud (HIP 64837, $d = 81$ pc and HIP 65178, $d = 128$ pc) and only HIP 64837 shows evidence for absorption. A third star, HIP 64925 ($d = 101$ pc), also evidence for the absorption, however this star is somewhat more distance from the cloud (see Fig. 4). Together, this suggests that the cloud is at a distance of $D_C < 81$ pc, although the nearby star HIP 65178 at $d = 128$ pc does not show absorption possibly due to fragmentary small scale cloud morphology. The velocities of the Na absorption lines ($V_{\text{LSR}} = -1.4$ km s $^{-1}$) and CO emission lines ($V_{\text{LSR}} = -8.3$ km s $^{-1}$) are again significantly discrepant, although they are within the errors of the absorption resolution. We find, that the absorption and emission spectra presented here suggest a complex multi-component spatial and kinematic distribution of clouds B and C.

4.2. Natal clouds of the TW Hya association

Considering the region encompassing TWA members that is not contaminated from the Galactic plane dust emission, $267^\circ < l < 310^\circ$ and $16^\circ < b < 35^\circ$, we find that only $\sim 3\%$ or 23 deg^2 shows a dust $E(B-V) > 0.15$ mag. The survey data presented in this report samples 1.94 deg^2 (excluding cloud A), showing CO in emission at only 8.5% of the observed positions. We can extrapolate this detection ratio to regions where $E(B-V) > 0.15$ mag, and estimate that 1.9 deg^2 will show CO in emission. Assuming a typical CO intensity of 0.5 K km s^{-1} and a molecular hydrogen column density of $8 \times 10^{19} \text{ cm}^{-2}$, we further estimate that the total molecular mass throughout the region defined above is $\lesssim 3 M_\odot$.

We can also estimate the mass of original pre-stellar molecular cloud; assuming a total current stellar mass of $\sim 16 M_\odot$ (Tachihara et al. 2003) and a star-formation efficiency of 3% (Tachihara et al. 2002), yields a pre-stellar molecular cloud mass of $540 M_\odot$. As such, less than 1% of the original cloud mass remains since the most recent TWA star formation, approximately 1 Myr ago. This is a considerably short dissipation timescale, in comparison to other nearby SFRs; Tachihara et al. (2001) noted that most T Tauri stars younger than 5 Myr found in Lupus and Chamaeleon, are within a few pc of the associated molecular clouds. They also note that small isolated clouds may also have been dissipated rapidly by nearby OB associations.

The present velocity dispersions of the candidate TWA natal molecular clouds are too high to be bound, suggesting that they may have been recently disturbed by some

external event. In the following, we present scenarios that may result in the observed and anomalously high velocity dispersions of the candidate TWA molecular clouds.

4.2.1. Scenario I

Careful analysis of kinematic data suggest that both the TWA and η Cha cluster formed from the Sco-Cen giant molecular cloud (GMC) at a distance of ~ 150 pc (Mamajek et al. 2000). Over the last ~ 10 Myr, they have been moving away from the Sco-Cen complex and are presently separated from the Lower Centaurus Crux (LCC) subgroup by 50-100 pc. The Sco-Cen GMC was later evacuated by stellar winds and/or SN explosion forming the giant “Loop I bubble” HI shell (de Geus 1992). The progenitor of the η Cha cluster may have been dispersed by the same SN responsible for forming the Loop I bubble.

4.2.2. Scenario II

TWA is within 110 pc of the sun, and is inside a low-density plasma region that fills the local bubble, observed as isotropic soft X-ray radiation (e.g. Tanaka & Bleeker 1977). The Pleiades moving group is a nearby OB association that may have been the source of a SN explosion in the last ~ 1 Myr, or of 3 SNe explosions in the last 5 Myr (Berghöfer & Breitschwerdt 2002). The shock wave from these events may be responsible enhancing the dissipation of the TWA natal molecular clouds, however the Pleiades moving group is large, with a scale of ~ 100 pc, and as such the relative proximity of the SN events to TWA is unclear, furthermore, no candidate SNe of such an explosion has yet been identified.

More accurate measurements of the proper motions, distances and radial velocities of both the TWA-member stars and candidate remnant molecular clouds, are crucial to refine and discriminate between these scenarios, as would search for any remnants of any SNs in the Pleiades moving group.

5. Summary

We have conducted a search for remnant clouds associated with the formation of TW Hya association in both CO emission, and Na absorption. We find that CO emission is detected towards three peaks of IR brightness, clouds A, B and C. Cloud A is relatively bright in CO emission and shows strong emission in IR, whereas clouds B and C are weaker by more than a factor of 3, and show a much more fragmentary distribution of CO emission. We reject the association of cloud A to the TWA, on the basis of a lack of a detection of Na absorption lines which indicate that it is much more distant than the TWA. Na absorption of Hipparcos targets help to constrain the distances of clouds B and C as that only a small fraction of the ISM has a distance less than 100 pc. Using a statistical approach, we estimate the total amount of molecular gas in this region is less than a few solar masses, and conclude that most of the natal molecular clouds associated with TWA has already dissipated with an unusually fast dissipation time scale, enhanced perhaps, by an external and energetic disturbance, or kinetic segregation with proper

motion of the member stars.

We are grateful to all the staff of the European Southern Observatory for their great hospitality. We thank Erik Muller for reading through the text. KT thanks financial support from JSPS (Japanese Society for the Promotion of Science). This work was supported by The 21st Century COE Program: Origin and Evolution of Planetary System of MEXT of Japan.

References

- Berghöfer, T. W., & Breitschwerdt, D. 2002, *A&A*, 390, 299
 Bohlin, R. C., Savage, B. D., & Drake, J. F. 1978, *ApJ*, 224, 132
 Dame, T. M., Hartmann, D., & Thaddeus, P. 2001, *ApJ*, 547, 792
 de Geus, E. J. 1992, *A&A*, 262, 258
 Foster, P. N., & Boss, A. P. 1996, *ApJ*, 468, 784
 Frink, S. 2001, *ASP Conf. Ser. 244: Young Stars Near Earth: Progress and Prospects*, ed. R. Jayawardhana & T. Greene (San Francisco: Astronomical Society of the Pacific), 16
 Hunter, S. D., et al. 1997, *ApJ*, 481, 205
 Jensen, E. L. N., Cohen, D. H., & Neuhäuser, R. 1998, *AJ*, 116, 414
 Kastner, J. H., Zuckerman, B., Weintraub, D. A., & Forveille, T. 1997, *Science*, 277, 67
 Mamajek, E. E., Lawson, W. A., & Feigelson, E. D. 1999, *ApJL*, 516, L77
 Mamajek, E. E., Lawson, W. A., & Feigelson, E. D. 2000, *ApJ*, 544, 356
 Mizuno, A., et al. 1998, *ApJL*, 507, L83
 Mizuno, A., Yamaguchi, R., Tachihara, K., Toyoda, S., Aoyama, H., Yamamoto, H., Onishi, T., & Fukui, Y. 2001, *PASJ*, 53, 1071
 Neuhäuser, R. 1997, *Science* 276, 1363
 Neuhäuser, R., Guenther, E. W., Petr, M. G., Brandner, W., Huélamo, N., & Alves, J. 2000, *A&A*, 360, L39
 Schlegel, D. J., Finkbeiner, D. P., & Davis, M. 1998, *ApJ*, 500, 525
 Tachihara, K., Toyoda, S., Onishi, T., Mizuno, A., Fukui, Y., & Neuhäuser, R. 2001, *PASJ*, 53, 1081
 Tachihara, K., Onishi, T., Mizuno, A., & Fukui, Y. 2002, *A&A*, 385, 909
 Tachihara, K., Neuhäuser, R., Frink, S., & Guenther, E. 2003, *Astronomische Nachrichten*, 324, 543
 Tachihara, K., Neuhäuser, R., Kun, M., & Fukui, Y. 2005, *A&A*, 437, 919
 Tanaka, Y., & Bleeker, J. A. M. 1977, *Space Science Reviews*, 20, 815
 Torres, G., Guenther, E. W., Marschall, L. A., Neuhäuser, R., Latham, D. W., & Stefanik, R. P. 2003, *AJ*, 125, 825
 Webb, R. A., Zuckerman, B., Platais, I., Patience, J., White, R. J., Schwartz, M. J., & McCarthy, C. 1999, *ApJL*, 512, L63
 Webb, R. A. 2001, in *ASP Conf. Ser. 244: Young Stars Near Earth: Progress and Prospects*, ed. R. Jayawardhana & T. Greene (San Francisco: Astronomical Society of the Pacific), 10
 Zuckerman, B., Webb, R. A., Schwartz, M., & Becklin, E. E. 2001, *ApJL*, 549, L233